

F.L. Lewis, Fellow IEEE, Fellow IFAC, Fellow UK InstMC
 Moncrief-O'Donnell Endowed Chair
 Head, Controls & Sensors Group

Automation & Robotics Research Institute (ARRI)
 The University of Texas at Arlington

Structural Health Monitoring



<http://ARRI.uta.edu/acs>
 lewis@uta.edu



SHM

Worden et al. 2009

Rytter's Levels:

- *Level 1.* (Detection.) The method gives a qualitative indication that damage might be present in the structure.
- *Level 2.* (Localization.) The method gives information about the probable position of the damage.
- *Level 3.* (Assessment.) The method gives an estimate of the extent of the damage.
- *Level 4.* (Prediction.) The method offers information about the safety of the structure, e.g. estimates a residual life.

classification

Machine Learning

- Classification, i.e. the association of a class or set label with a set or vector of measured quantities. The set of observations may be sparse and/or noisy.
- Regression, i.e. the construction of a map between a group of continuous input variables and a continuous output variable on the basis of a set of (again, potentially noisy) samples.
- Density estimation, i.e. the estimation of probability density functions from samples of measured data.

Methods of Learning
 supervised
 unsupervised
 reinforcement

Machine learning and SHM

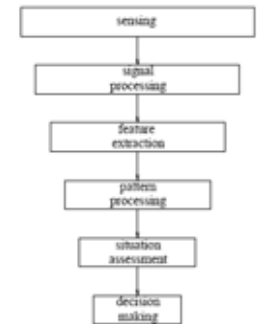
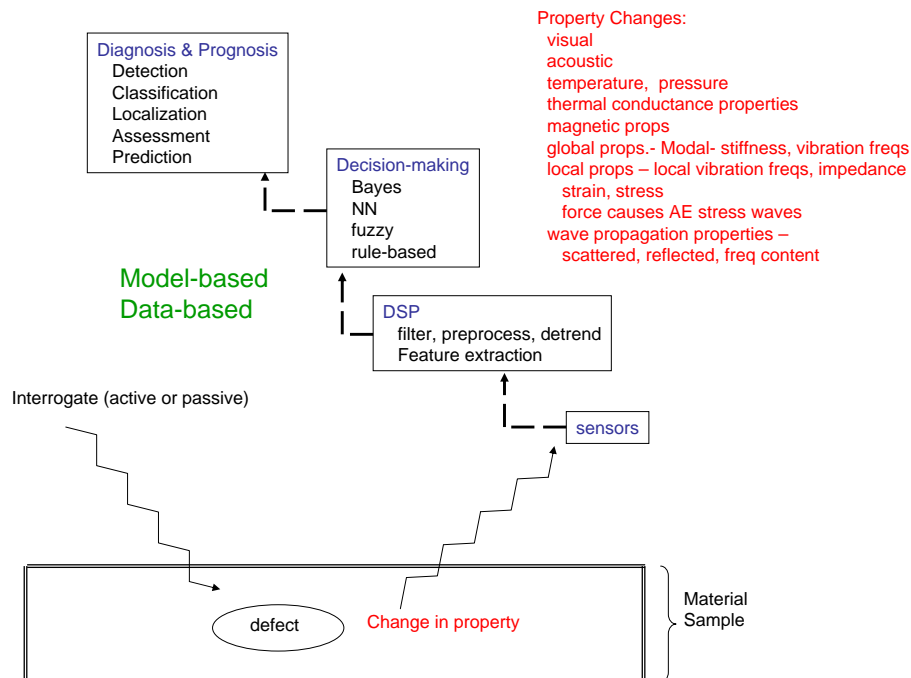


Figure 1. Waterfall model.



Fault Types

Composites

Matrix (resin) crack
 Delamination
 Fibre breaks

Metals

Material Defects
 Corrosion
 Crack
 Fatigue

System Defects
 Rivet Failure
 Surface Ice

Detection Methods

Vibration (LF- wavelength >> plate thickness)
 global- LF - changes in structural props- stiffness, vibr. freqs.
 local- HF - changes in res. freqs., impedance

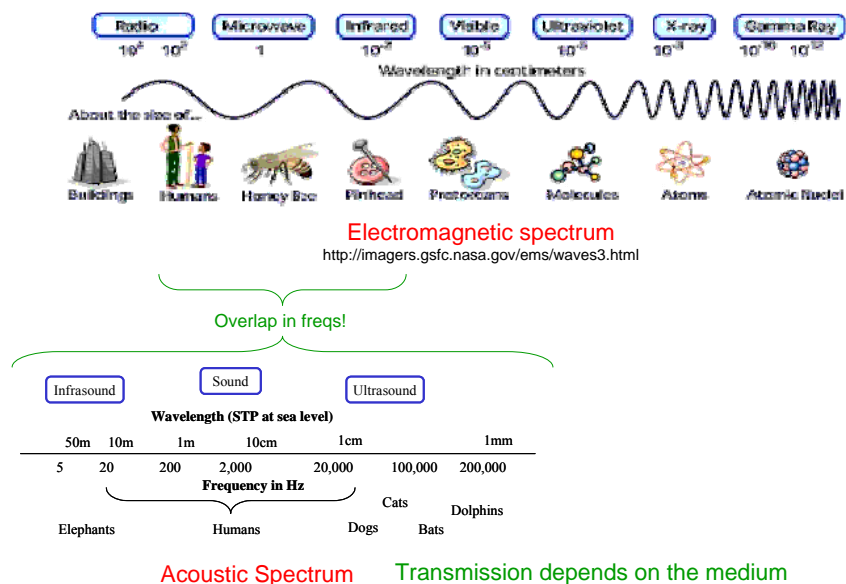
Sonic

Ultrasound (HF- wavelength << thickness)
 Acoustic Emission (mid freq.- wavelength ~ thickness)
 Wave Propagation (single freq waves)

Strain, Stress

X-Ray
 Visual
 Thermal
 Magnetic

Sensor Modalities



Sensors Based on Physical Transduction Principles

Mechanical Sensors

Piezoresistive Effect converts an applied strain to a change in resistance
Piezoelectric Effect converts an applied stress (force) to a potential difference. **PZT**
Capacitive Sensors convert displacement (force) into change in capacitance

Magnetic and Electromagnetic Sensors

do not require direct physical contact
Hall Effect. Magnetic field applied perpendicular to current flow causes induced voltage
Magnetic Field Sensors detect metallic objects
Eddy Current Sensors use magnetic probe coils to detect defects in metallic structures

Thermal Sensors

measure temperature or heat flux
Thermo-Mechanical Transduction. Heat causes thermal expansion
Thermoresistive Effects. Resistance R changes with temperature T
Thermocouples. Junctions of two different metals at different temperatures causes current flow
Resonant Temperature Sensors. Temp change in some materials causes a change in resonant frequency

Optical Transducers.

Convert various properties to light
Optical fiber interferometers and gratings— changes in length (strain), temp. cause changes in phase
Optical fiber accelerometers based on time of flight

Acoustic Sensors

Ultrasound. High Frequency. Can penetrate structures. Reflected and scattered from defects
Acoustic Wave Sensors
 surface acoustic wave (SAW), thickness-shear mode (TSM), flexural plate wave (FPW), or acoustic plate mode (APM)

F.L. Lewis, "Wireless Sensor Networks," in *Smart Environments: Technologies, Protocols, Applications*, Chapter 2, ed. D.J. Cook and S.K. Das, Wiley, New York, 2005.

PZT - Lead zirconate titanate

Piezoelectric

Sensor- develops a **voltage** difference across two of its faces when compressed
Actuator- physically changes shape when an external electric field is applied

Pyroelectric

Heat Sensor- Develops a voltage difference across two of its faces when it experiences a temperature change.

TEMP. COMPENSATION

Ferroelectric-

Has a spontaneous **electric polarization** (**electric dipole**) which can be reversed in the presence of an electric field.

Interrogation / Interaction Modalities

Group 1

X-ray
 Visual
 Coherent Optics
 Fiber optics – no EMI, lightweight, low noise, high BW
 Interferometry
 Fiber Bragg Grating - FBG

Thermography - IR
 Magnetics

Eddy current
 a coil induces eddy currents in a conductive sample
 defects cause change in the impedance of the sample

Group 2- Sonic

Sound propagation depends on the medium
Defects scatter or reflect sound waves

Ultrasound HF (5 MHz)

wavelength << thickness
short prop. Distance
a single excit. freq.

Acoustic Emission AE Mid freq (100 kHz-2 MHz)

wavelength ~ thickness
substantial prop. dist. (a few m.)
multiple excitation freqs. (e.g. white noise)

Lamb Wave is AE with a single excit. freq.

Group 3- Vibration Wavelength >> thickness

Monitor vibration signature- pattern recognition

LF (20 Hz – 20 kHz)

Global- changes in physical props.
Modal parameters (stiffness, res. freq.)

HF (100 kHz – 1 MHz)

Local- changes in frequency content
EM impedance
PZT sensors

Group 4- Strain, Stress

Force on defect causes AE stress waves

Lamb Waves wavelength ~ thickness

wikipedia

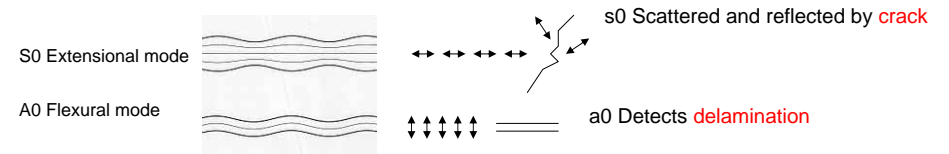
Irradiate entire thickness
Propagate substantial distances

Elastic waves that propagate in a solid thin plate

2-D Wave equation

$$\nabla^2 \phi = \frac{1}{c^2} \frac{\partial^2 \phi}{\partial t^2}$$

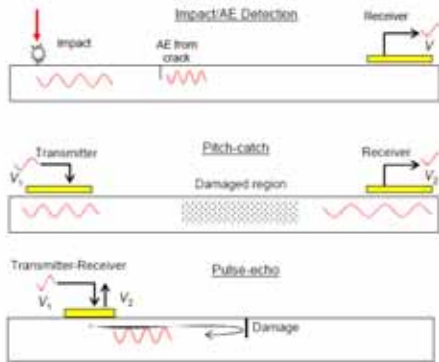
solutions split into two sets of waves-
symmetric & antisymmetric



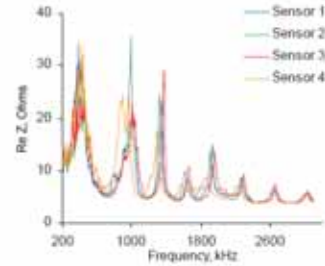
A major challenge and skill in the use of Lamb waves for ultrasonic testing is the generation of specific modes at specific frequencies that will propagate well and give clean return "echoes". This requires careful control of the excitation and identification of the correct waves.

How are Piezo actuator/sensors used in SHM ?

Propagating Lamb waves



E/M Impedance



Actuation / Interrogation

Active vs. Passive

Passive vibration monitoring-
in-flight aircraft vibration freqs are very low
successful in a boat hull monitoring application

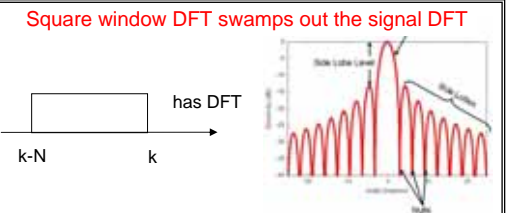
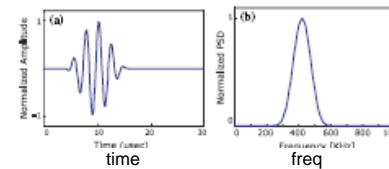
Active -

PZT actuator

Eddy-coil EM actuator
discharges capacitor through a coil, induces pulsed magnetic field in conductive sample,
generates a force
needs 1-10 J

Actuator interrogation signals

Burst sinusoids



FFT of burst sinusoids with:

Square window

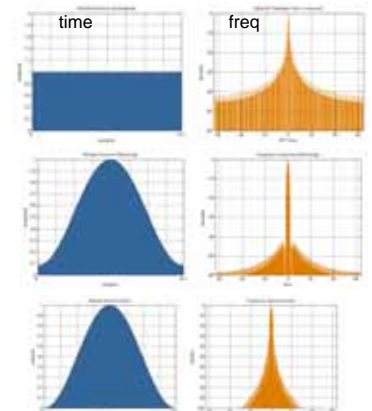
$$w(n) = 1$$

Hamming window

$$w(n) = 0.54 - 0.46 \cos\left(\frac{2\pi n}{N-1}\right)$$

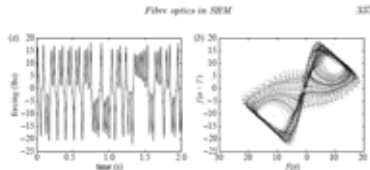
Hann window

$$w(n) = 0.5 \left(1 - \cos\left(\frac{2\pi n}{N-1}\right)\right)$$



Chaotic Interrogator Actuation

Todd et al. 2009



Actuation by Lorenz Signal

Figure 14. (a) Driving signal and (b) corresponding phase space representation.

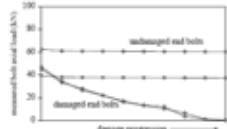


Figure 15. Progression of measured axial load for each of the instrumented bolts.

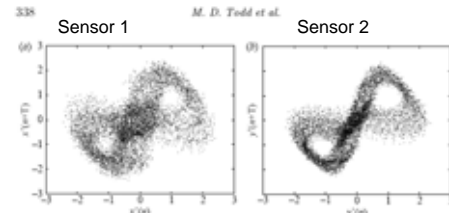


Figure 16. Attractor reconstructions for (a) sensor 1 and (b) sensor 2 data for undamaged case.

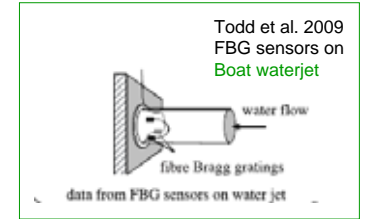
Signals received at sensors

Actuator and Sensor Locations

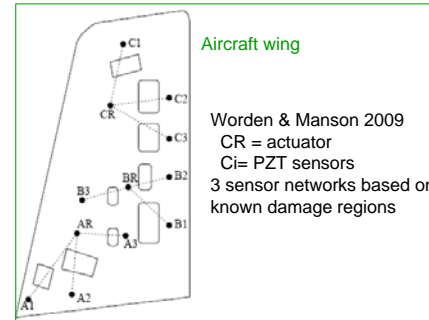
c.f. human nervous system proprioceptors

Based on Physical Models
FEA or dynamics model
Based on Engineering Knowledge

Deploy at Hot Spots
Deploy over a Large Area-
limits the frequencies and interrogation methods



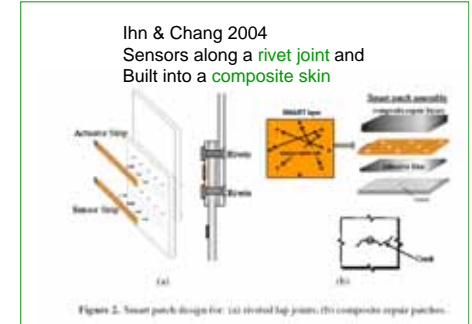
Todd et al. 2009
FBG sensors on
Boat waterjet



Aircraft wing

Worden & Manson 2009
CR = actuator
Ci = PZT sensors
3 sensor networks based on known damage regions

No methodical procedures



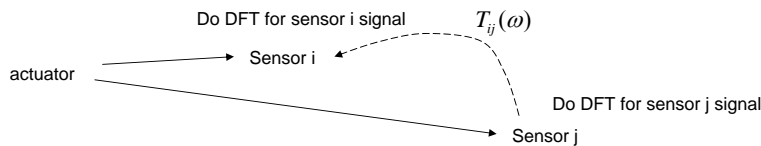
Ihn & Chang 2004
Sensors along a rivet joint and
Built into a composite skin

Features

- Time moments
- Frequency domain properties-
Resonant freqs, sidebands
Power content in specific frequency bands
Transmissibilities
- Strain, stress

Transmissibility from sensor j to sensor i

$$T_{ij}(\omega) = \frac{PSD_i(\omega)}{PSD_j(\omega)}$$



Time-Varying Frequency Content

Short Time Fourier Transform – Windowed DFT

Must select window length
Must use good window w(n) - Hamming, Hann

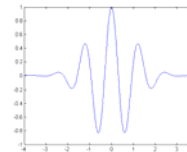
$$X(k, t) = \sum_{n=t-(N-1)}^t x(n)w(t-n) e^{-j2\pi(k-1)(n-1)/N}$$

Wavelet

Does not need window
Multi-resolution analysis

Basic or mother wavelet

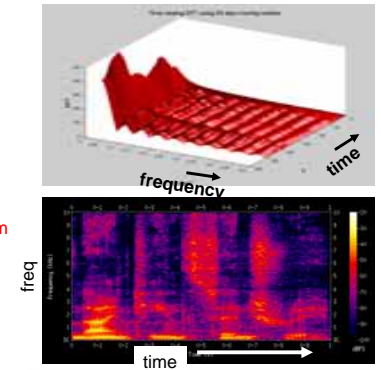
$$\psi(t) = 2 \operatorname{sinc}(2t) - \operatorname{sinc}(t) = \frac{\sin(2\pi t) - \sin(\pi t)}{\pi t}$$



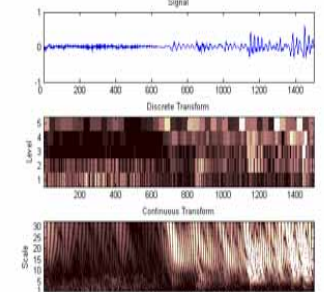
$$Wf(u, s) = \int f(t) \frac{1}{\sqrt{s}} \psi^* \left(\frac{t-u}{s} \right) dt = (f, \psi_{u,s})$$

Hilbert-Huang Transform (HHT)

STFT Spectrogram



Wavelet xform Sacleogram



Fault detection & Identification

Model-Based

make physical model using FEA or physics-based methods
 determine comparison metric
 look for departures of real measured data from the model

Data-Based

based on moments, freq response, or statistics
 establish normal operating limits based
 establish abnormality thresholds
 departures indicate faults

Both methods look for departures from the norm
 this means **Statistical Pattern Recognition**
 preprocessing of data, filter, detrend
 outlier rejection



Physical Modeling

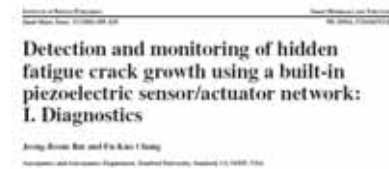
e.g. Deterministic Crack Propagation Models

- Variations of available empirical and deterministic fatigue crack propagation models are based on Paris' formula:

$$\frac{da}{dN} = C_o (\Delta K)^n$$

Where:

- a = instantaneous length of dominant crack
- N = running cycles
- C_o, n = material dependent constants
- ΔK = range of stress intensity factor over one loading cycle



Ihn and Chang 2004

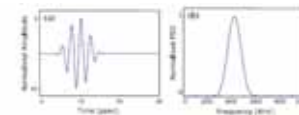


Figure 2. The diagnostic signal waveforms at a driving frequency of 420 kHz: (a) A windowed burst signal with five cycles. (b) The frequency spectrum (power spectral density).

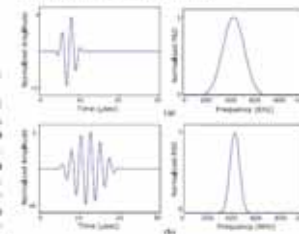


Figure 3. Effects of varying the number of cycles on burst waveforms (at a driving frequency of 420 kHz): (a) A burst signal with five cycles. (b) A burst signal with ten cycles.

Lamb Waves

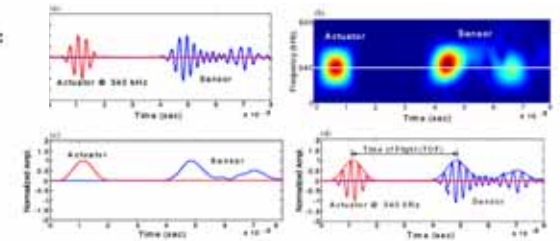


Figure 4. Extracting time of flight information.

Must focus on ONE frequency

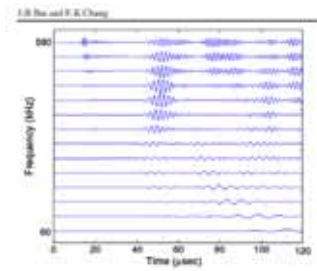
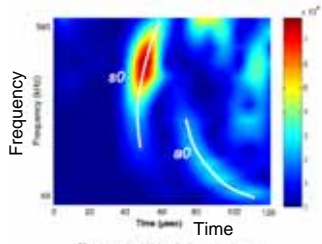
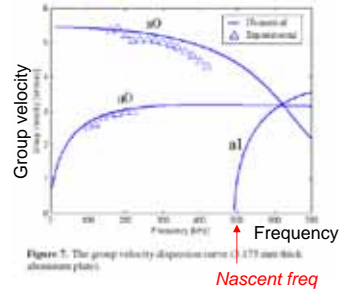


Figure 5. The received signal collected.

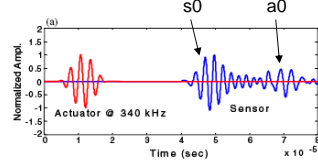
Where is the right Lamb wave?



Group velocity Dispersion
From FEA for the specific material



s0 arrives before a0 below 600kHz



$$\text{Damage index (DI)} = \left(\frac{\int_a^b |S_{sc}(\omega_0, t)|^2 dt}{\int_a^b |S_b(\omega_0, t)|^2 dt} \right)^m$$

Use s0 for cracks
Use a0 for composite delamination

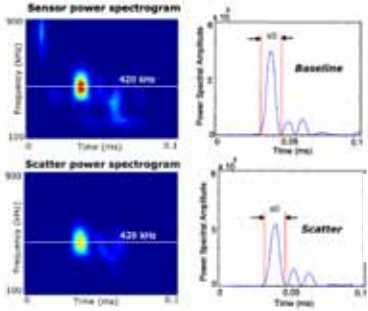


Figure 9. Energy contents in the s0 mode.

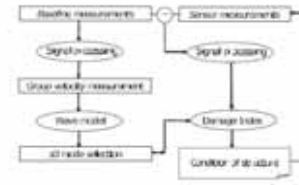


Figure 12. The crack detection scheme.

Optimal sensor location wrt crack

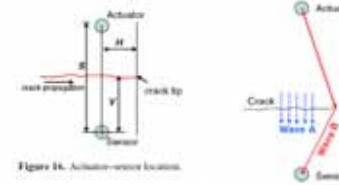


Figure 14. Actuator-sensor location.

$$\text{Damage index (DI)} = \left(\frac{\int_a^b |S_{sc}(\omega_0, t)|^2 dt}{\int_a^b |S_b(\omega_0, t)|^2 dt} \right)^m$$

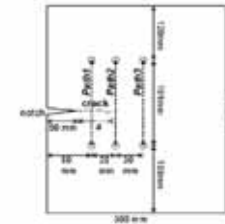


Figure 13. A 1.175 mm thick aluminum plate with a 70 mm machine notch.

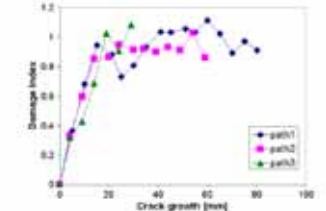


Figure 15. Damage index versus crack growth with $\omega_0 = 20$ kHz for path 1, 40 kHz for path 2 and 70 kHz for path 3.

Smart Suitcase

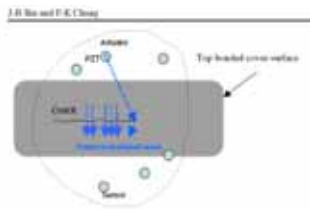


Figure 1. The wave propagation configuration for crack detection.

Accellent Technol. Smart patch

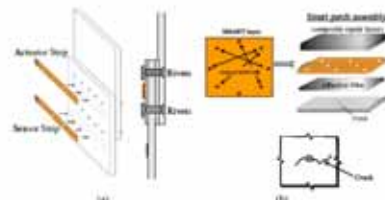


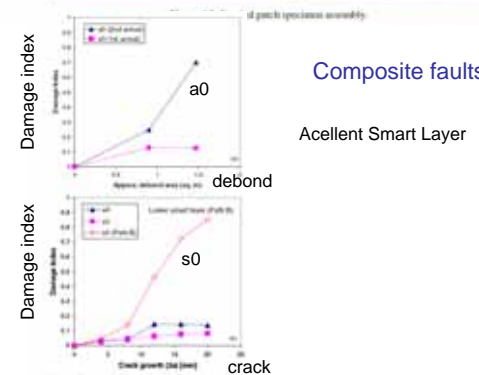
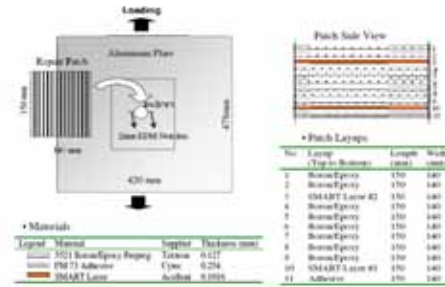
Figure 2. Smart patch design for: (a) rivet lap joints; (b) composite repair patches.

Rivet failure

Ihn and Chang 2004



Figure 1. The built-in diagnostic system.



Composite faults

Accellent Smart Layer

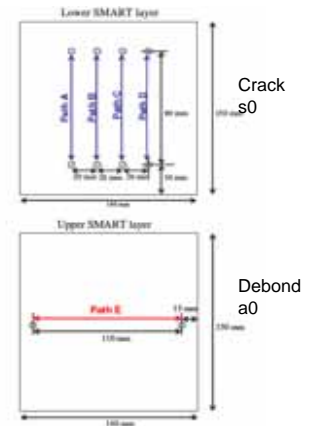


Figure 14. SMART layers with diagnostic paths.

TECHNICAL NOTE

Structural health monitoring of composite structures using Lamb wave tomography

S Mahadev Prasad, Krishnan Balasubramanian and C V Krishnamurthy

Tomography- imaging by sections using wave energy

2D or 3D images

- x-ray CT
- gamma
- electron

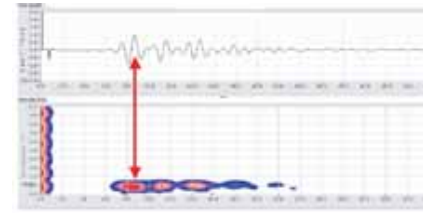
Reconstruction algorithms

- filtered back projection
- iterative reconstruction
- ART- algebraic reconstruction techniques (Kaczmarcz algorithm)



Cardiac CT scan

wikipedia



s0 energy- compute energy up to MAXIMUM Peak
 Use RMS value for tomographic reconstruction

Freq = 500 kHz

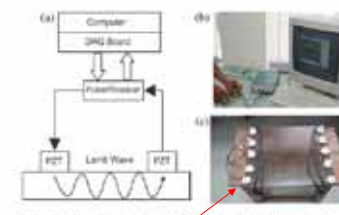


Figure 3. Experimental setup: (a) Schematic; (b) instrumentation and (c) 5 x 5 cross-hole setup

Sticky gum to hold sensors?

Split plate into a uniform grid
 Mount sensors at grid points
 400 sensors!

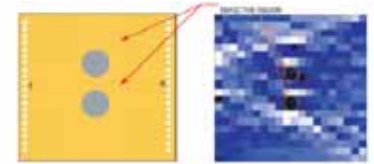
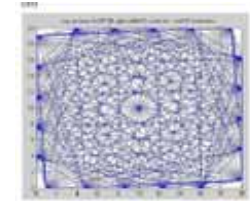


Figure 6. Tomogram of quasi-isotropic laminate with two defects.

Improved sensor placement



Uniform angular sampling of plate with few sensors

Neural network method based on a new damage signature for structural health monitoring

Shenfang Yuan^a, Lei Wang, Ge Peng

Used Kohonen NN to classify damage

Wide band Lamb waves

Excitation – rectangular impulse 10 microsec wide
 Excites Lamb waves covering a broad frequency spectrum

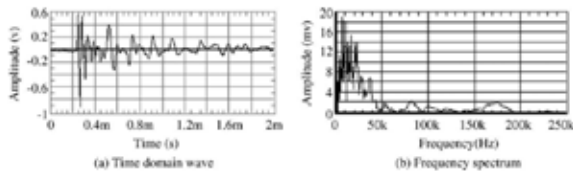


Fig. 2. Wide-band Lamb wave signal excited in honey-comb sandwich beam and its frequency spectrum.

Compensate for Propagation- amplitude A with distance x

$$A = A_0 e^{-\alpha x} \quad (1)$$

where A=the peak amplitude of the monitored signal, x=the distance of signal propagation, α =attenuation coefficient, A_0 =the initial peak amplitude value at the point of excitation. To reduce the propagation distance effect on peak value, a new signature can

Application of Smart Structures to Aircraft Health Monitoring
 G.A. Hickman, J.J. Gerardi and Y. Feng
 Journal of Intelligent Material Systems and Structures 1991; 2, 411
 DOI: 10.1177/1045389X9100200308

Hickman et al. 1991

Select Features?

LF vibration 1-5 kHz

Defects cause energy redistribution in freq. spectrogram

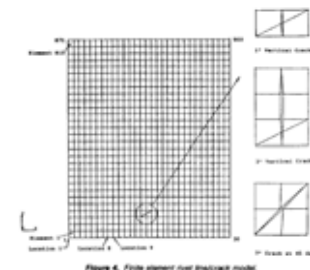


Figure 4. Finite element model of the aircraft model.

FEA

Rivet removal and cracks both lower the HF content

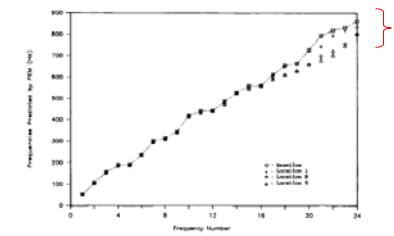


Figure 5a. Frequency variation with rivets removed

G. A. HICKMAN, J. J. GERARDI AND Y. FENG

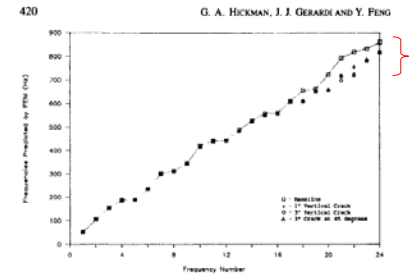


Figure 5b. Frequency variation with crack damage.

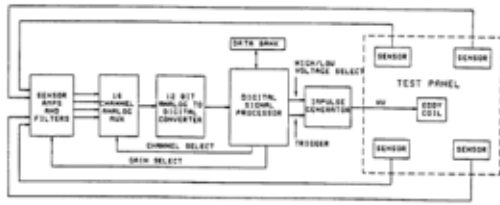


Figure 2. Block diagram of the HMS system.

Compute features for each sensor

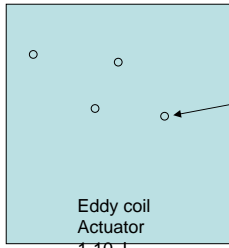
Table 1. Features extracted from piezoelectric sensor signals.

Feature	Description
1	local damping coefficients
2	one-half of the modulation signal period
3	standard deviation of signal
4	kurtosis of signal
5	skewness of signal
6	time at 90% decay
7	amplitude ratio of two biggest peak values
8	frequency of the biggest peak value
9	frequency difference of two biggest peaks
10	2nd largest peak value
11	partial power in relevant frequency bands between 1-10 kHz
12	ratio of smallest and largest partial power
13	number of peaks exceeding a given threshold
14	frequency at which 25%, 50%, and 75% of accumulated power was observed
15	transfer ratio of partial power in frequency bands between 1-10 kHz

Best Features:
Energy distribution- Power in specific freq bands

24" sq. plate, 0.08" thick

Screws around edges



Eddy coil Actuator
1-10 J

Sensor placement determined experimentally!

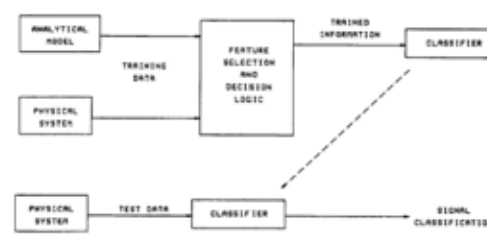


Figure 3. Generalized classification procedure.

NN classification?

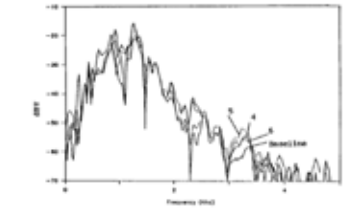
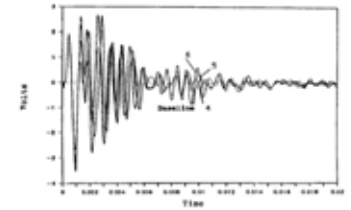


Figure 9. River line ground tests using eddy-coil impulse excitation: river line 4, 5, 6 and baseline.

Features-
Energy distribution- Power in specific freq bands

1-1.5 kHz
1.5-3 kHz

Aircraft Monitoring

Rivet failures
Cracks
icing

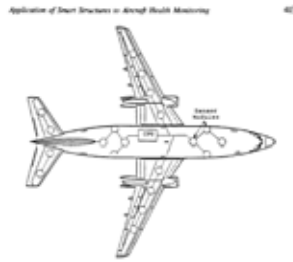


Figure 1. Health monitoring system concept.

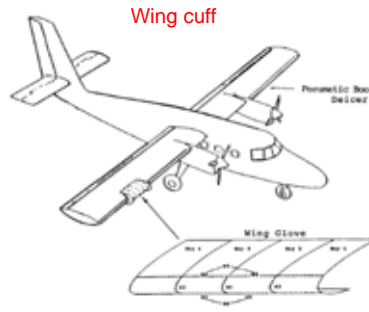


Figure 7. Twin Otter wing cuff testbed.

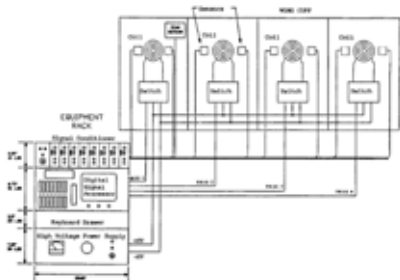


Figure 8. HMS Twin Otter hardware test configuration.

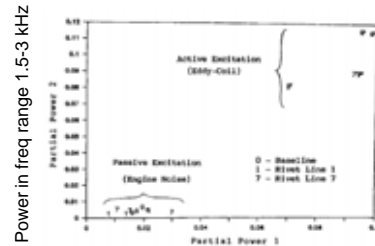


Figure 11. Rivet line flight test separability comparison for wing cuff.

Power in freq range 1-1.5 kHz

The application of machine learning to structural health monitoring

Keith Worden and Graeme Manson
Phil. Trans. R. Soc. A 2007 365, 515-537
doi: 10.1098/rsta.2006.1938



Figure 2. Gust aircraft and acquisition system.

1. Damage detection

K. Worden and G. Manson

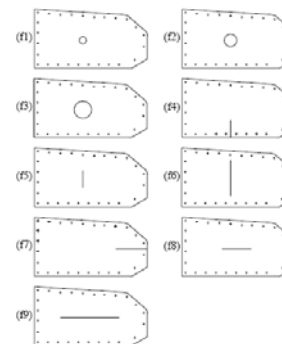
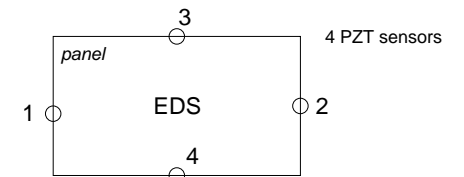


Figure 3. Schematic of damage states.

Damaged panels



EDS= Electrodynamic shaker
LF EM Vibration at 1-2 kHz
Compute DFT

Transmissibility from sensor j to sensor i

$$T_{ij}(\omega) = \frac{PSD_i(\omega)}{PSD_j(\omega)}$$

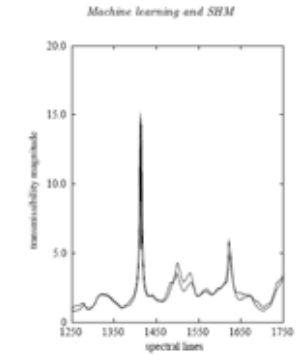


Figure 4. Examples of averaged transmissibility measurements.

Features = power in specific freq bands

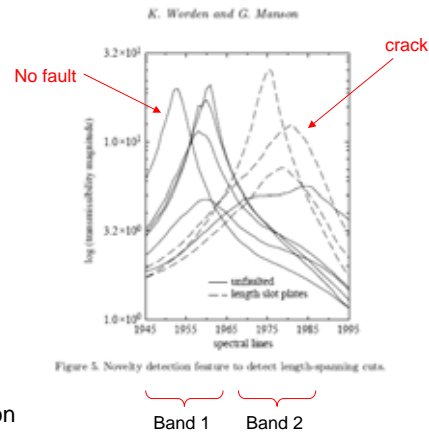


Figure 5. Novelty detection feature to detect length-spanning cuts.

Classification and departure detection
 NN
 clustering (K-means, NN)
 outlier analysis using norm distance measure
 Training data Set and Validation Set
 Unsupervised learning for fault detection

2. Damage Location

Network of sensors

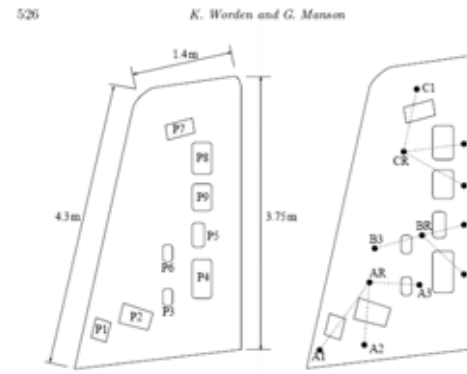


Figure 8. Schematic of the starboard wing inspection panels and transducer locations.

CR = PZT actuator
 Ci = PZT sensors

Actuator and sensor locations based on KNOWN possible fault locations

4 networks with
 1 actuator and 3 sensors

Damage = remove panels
 NN MLP classifier – competitive learning

Supervised learning for fault classification or fault location

Bragg grating-based fibre optic sensors in structural health monitoring

By MICHAEL D. TOBE^{1,2}, JONATHAN M. NICHOLS²,
 STEPHEN T. TRICKY², MARK SEATER², CHRISTY J. NICHOLS²
 AND LAWRENCE N. VIRGIN²

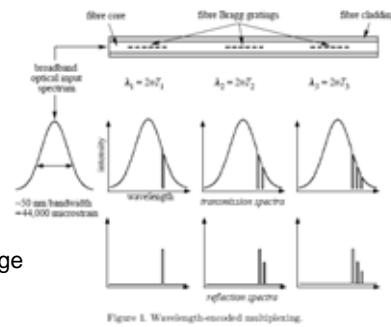


Figure 1. Wavelength-encoded multiplexing.

Fiber Bragg Grating – FBG
 Interrogate length scales in the mm range
 No EMI
 Lightweight
 Can be directly photo written into silica fiber using UV
 Embed inside composites

$$\lambda_r = 2nT \quad \text{about } 0.1\text{--}0.3 \text{ nm}$$

n = fiber core model index, T = grating period

Axial compression or tension changes T – can measure strain

Boat Hull Monitoring – passive wave excitation
 Joint Degradation – active excitation - EDS

Boat Hull Monitoring

A-K = 11 sensor arrays
 56 sensors in all
 Rosette = 3-D sensor?

Passive excitation

Sensor placement
 hull monitoring
 waterjet monitoring

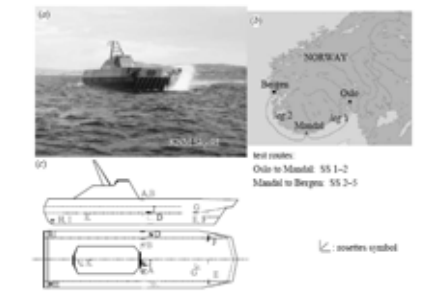


Figure 8. (a) A photograph of the KRM Sjøtid, (b) the test routes and (c) the sensor locations; rosettes are indicated by small square symbols.

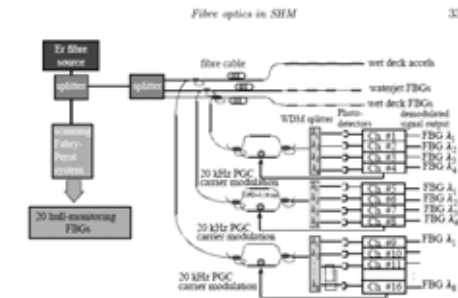


Figure 9. Complete ship monitoring system, including both SFP and WDM architectures required for hull and waterjet monitoring.

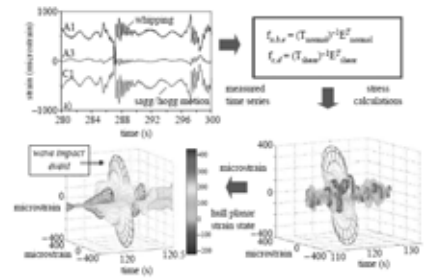


Figure 10. Characterization of primary boat motions and using rosettes to determine real-time state of strain in hull.

Ultrasonic NDE of composite material structures using wavelet coefficients

S. Legendre*, J. Goyette, D. Massicotte

$$Wf(u, s) = \int f(t) \frac{1}{\sqrt{s}} \psi^* \left(\frac{t-u}{s} \right) dt = \langle f, \psi_{u,s} \rangle$$

Feature selection
Select specific levels only

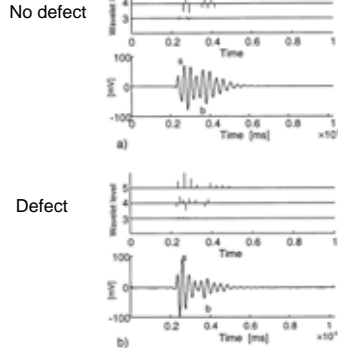


Fig. 3. Feature extraction from ultrasonic signals $N = 3, L = 5$ and $M_j = j = 3, 4, 5$ (Eq. (8)): (a) defect-free region; and (b) region with defect.

Discrete wavelet transform Set scale factor equal to 2^j

tions at the scale 2^j . In that case, the orthonormal basis is defined by

$$\left\{ \phi_{j,n}(t) = \frac{1}{\sqrt{2^j}} \psi \left(\frac{t - 2^j n}{2^j} \right) \right\}_{(j,n) \in \mathbb{Z}^2} \quad (4)$$

for $n = 1, 2, \dots, N$ and $j = 1, 2, \dots, J$ with $N = 2^j$. The signal $f(t)$ can be decomposed over this basis

$$f(t) = \sum_{j=1}^J \sum_{n=1}^N \langle f, \phi_{j,n} \rangle \phi_{j,n}(t) \quad (5)$$

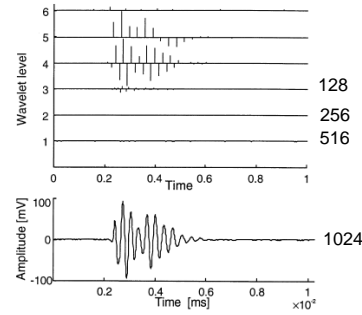


Fig. 2. Wavelet levels of an ultrasonic A-scan signal generated in a glass/epoxy composite structure compared to the original signal in the lower part of the figure.

SAW Devices as Wireless Passive Sensors

L. Reindl, G. Scholl, T. Ostertag, C.C.W. Ruppel, W.-E. Bulst, and F. Seifert*

1996 IEEE Ultrasonics Symp.

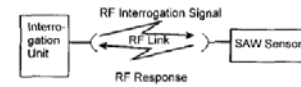


Fig. 1. Schematic drawing of a wireless sensor system based on passive SAW sensors.

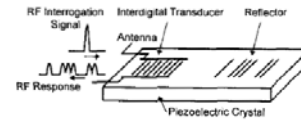


Fig. 2. Schematic layout of a passive SAW device used for identification and sensor applications.

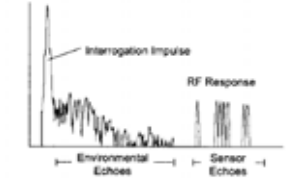


Fig. 3. Interrogation pulse, environmental echoes, and RF response of a SAW reflective delay line.

Gate this part = 1-2 micro sec

SAW + RFID

Interrogation freqs 434MHz = 5-10 m RFID range
2.5 GHz = 1-2 m RFID range

Changes in time delay and freq due to physical quantity $y(t)$

$$\tau(y_0 + \Delta y) = \tau(y_0) [1 + S_y \Delta y] \quad (1)$$

$$f(y_0 + \Delta y) = f(y_0) [1 - S_f \Delta y] \quad (2)$$

Sensitive to $y(t)$ = temp., displacement
 $y(t)$ = strain, force, accel. needs proper packaging

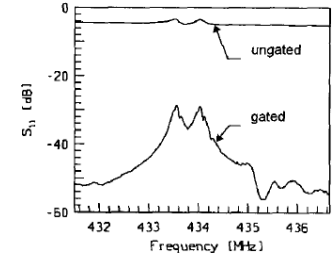
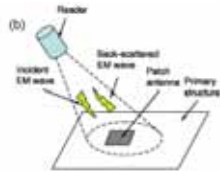


Fig. 6. Measured RF response of the resonator sensor (upper line: original frequency response, lower line: after gating in time domain).

Bio-inspired sensor skins for structural health monitoring

Haiying Huang, ME Dept, UTA

Uday Tata*, S Deshmukh*, J C Chiao*, Ronald Carter* and H Huang*



Patch Antenna

Strain causes Res freq shift

$$\frac{\Delta f}{f_0} = \frac{f_s - f_{s0}}{f_s} = \frac{L_{s0} + C_2 h_0}{L_{s0} + v_s C_2 h_0} \epsilon_L = C \epsilon_L$$

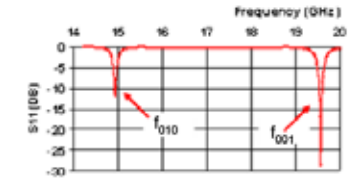


Figure 3. Simulated S_{11} of dual frequency patch antenna.

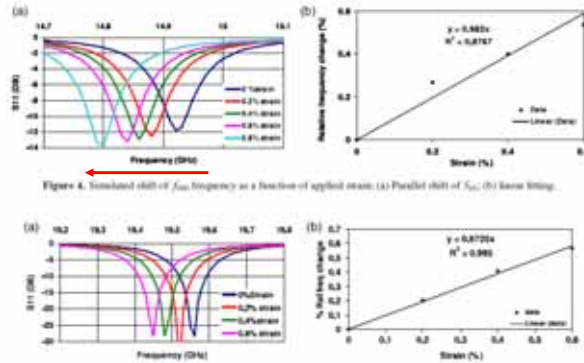


Figure 4. Simulated shift of f_{001} frequency as a function of applied stress: (a) Parallel shift of S_{11} ; (b) linear fitting.

Passive induction coupling-remote interrogation

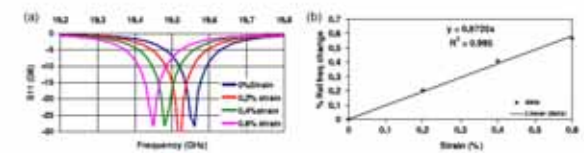
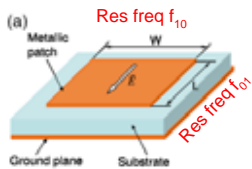


Figure 5. Simulated shift of f_{001} frequency as a function of applied stress: (a) Parallel shift of S_{11} ; (b) linear fitting.

Crack Monitoring

Haiying Huang, ME Dept, UTA

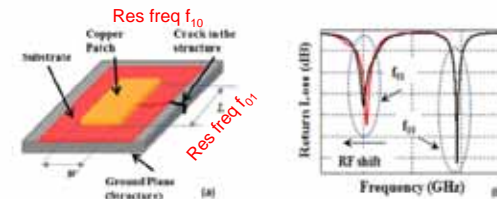


Figure 1: Principle of antenna sensor for crack monitoring: (a) Diagram of a patch antenna with width direction crack; (b) reduction of f_{01} frequency due to width direction crack.

